Clinical and Translational Radiation Oncology 40 (2023) 100602

Contents lists available at ScienceDirect

Clinical and Translational Radiation Oncology

journal homepage: www.sciencedirect.com/journal/clinical-and-translational-radiation-oncology

An exploratory analysis of MR-guided fractionated stereotactic radiotherapy in patients with brain metastases

Shouliang Ding [a,1], Biaoshui Liu [a,1], Shiyang Zheng [a,1], Daquan Wang [a], Mingzhi Liu [a], Hongdong Liu [a], Pengxin Zhang [a], Kangqiang Peng [b], Haoqiang He [b], Rui Zhou [a], Jinyu Guo [a], Bo Qiu [a], Xiaoyan Huang [a,**], Hui Liu [a,*]

[a] Department of Radiation Oncology, State Key Laboratory of Oncology in South China, Sun Yat-sen University Cancer Center, Guangzhou, China
[b] Department of Radiology, State Key Laboratory of Oncology in South China, Sun Yat-sen University Cancer Center, Guangzhou, China

ARTICLE INFO

Keywords:
Brain metastases
Fractionated stereotactic radiotherapy
Inter-fractional changes
MR-Linac
Adaptive radiotherapy

ABSTRACT

Purpose: To assess the feasibility and potential benefits of online adaptive MR-guided fractionated stereotatic radiotherapy (FSRT) in patients with brain metastases (BMs).
Methods and materials: Twenty-eight consecutive patients with BMs were treated with FSRT of 30 Gy in 5 fractions on the 1.5 T MR-Linac. The FSRT fractions employed daily MR scans and the contours were utilized to create each adapted plan. The brain lesions and perilesional edema were delineated on MR images of pre-treatment simulation (Fx0) and all fractions (Fx1, Fx2, Fx3, Fx4 and Fx5) to evaluate the inter-fractional changes. These changes were quantified using absolute/relative volume, Dice similarity coefficient (DSC) and Hausdorff distance (HD) metrics. Planning target volume (PTV) coverage and organ at risk (OAR) constraints were used to compare non-adaptive and adaptive plans.
Results: A total of 28 patients with 88 lesions were evaluated, and 23 patients (23/28, 82.1%) had primary lung adenocarcinoma. Significant tumor volume reduction had been found during FSRT compared to Fx0 for all 88 lesions (median −0.75%, −5.33%, −9.32%, −17.96% and −27.73% at Fx1, Fx2, Fx3, Fx4 and Fx5, $p < 0.05$). There were 47 (47/88, 53.4%) lesions being accompanied by perilesional edema and the inter-fractional changes were significantly different compared to those without perilesional edema ($p < 0.001$). Patients with multiple lesions (13/28, 46.4%) had more significant inter-fractional tumor changes than those with single lesion (15/28, 53.6%), including tumor volume reduction and anatomical shift ($p < 0.001$). PTV coverage of non-adaptive plans was below the prescribed coverage in 26/140 fractions (19%), with 12 (9%) failing by more than 10%. All 140 adaptive fractions met prescribed target coverage. The adaptive plans also had lower dose to whole brain than non-adaptive plans ($p < 0.001$).
Conclusions: Significant inter-fractional tumor changes could be found during FSRT in patients with BMs treated on the 1.5 T MR-Linac. Daily MR-guided re-optimization of treatment plans showed dosimetric benefit in patients with perilesional edema or multiple lesions.

Introduction

Stereotactic radiotherapy remains an effective treatment option for patients with brain metastases (BMs) [1,2]. To reduce the risk of brain necrosis while maintaining the disease control, fractionated stereotactic radiotherapy (FSRT) has been applied in patients with large/multiple brain lesions [3–7]. The variations of tumor size, geometry and position caused by therapy might lead to inadequate dose to target and increased radiation to normal tissue, which could affect the treatment efficacy in patients with large/multiple BMs. However, there were few studies that have assessed the necessity for re-planning during FSRT in BMs patients [8,9], and the optimal candidates for adaptive radiotherapy also

* Corresponding author at: Department of Radiation Oncology, Sun Yat-sen University Cancer Center, State Key Laboratory of Oncology in South China, 651 Dongfeng Road East, Guangzhou, Guangdong 510060, China.
** Co-corresponding author.
E-mail address: liuhuisysucc@126.com (H. Liu).
[1] Shouliang Ding, Biaoshui Liu and Shiyang Zheng contributed equally to this work.

https://doi.org/10.1016/j.ctro.2023.100602
Received 30 November 2022; Received in revised form 15 February 2023; Accepted 19 February 2023
Available online 23 February 2023

remained unclear.

Although the cone beam computed tomography (CBCT) guided stereotactic radiotherapy was commonly used in patients with BMs, efforts had been made to improve the accuracy of image registration. The high soft-tissue resolution magnetic resonance imaging (MRI) as imaging-guided technology is essential for FSRT to assure highly precise treatment delivery in patients with BMs. MRI remains the standard tool for diagnosis and assessment of BMs because of the excellent soft tissue resolution and offers functional sequences to investigate physiology [10–13]. Several studies reported notable changes in tumor volume and position during radiotherapy in patients with BMs by daily MRI scan [14,15]. Hence, the integration of MRI and linear accelerator (MR-Linac) is a novel option for this subgroup of patients [11,16,17] for it allows daily position verification and the delivery of adaptive radiotherapy [2,11,18].

Great attention has been paid to MR-Linac since it realized real-time image-guided adaptive radiotherapy [19–23]. MR-guided adaptive radiotherapy might provide new breakthroughs in normal tissue protection and disease control. We assumed that the online adaptive MR-guided FSRT could improve dosimetric accuracy by adjusting treatment plans according to inter-fractional anatomical changes. This study aimed to assess the feasibility and potential benefits of online adaptive MR-guided FSRT in BMs patients.

Methods and materials

Patient cohort and clinical data

A total of 28 consecutive patients with BMs treated with MR-guided FSRT on the 1.5 T MR-Linac [24] (Unity, Elekta AB, Stockholm, Sweden) from May 2021 to May 2022 were included in this study. All patients had received FSRT with a total dose of 30 Gy in 5 fractions daily. The eligibility criteria were as follows: patients with histologically or cytologically confirmed malignant tumors; ECOG score of 0–2; stable systemic and extracranial disease. Exclusion criteria included: conditions that were contra-indicatory to radiotherapy, such as recent myocardial infarction, active congestive heart failure, uncontrolled infectious disease or other serious medical or psychiatric illness; brain metastases were not visible on MRI T2 imaging were excluded since the Unity MR-Linac cannot offer contrast images and an inaccurate target delineation cannot been applied in online adaptive radiotherapy; contraindications for 1.5 T MR scan, such as claustrophobia, metal objects, pacemakers and an inability to tolerate a 30-minute treatment. This study was approved by the institutional ethics committee and all patients provided written informed consent prior to enrollment.

Patient pre-treatment workflow and QA

The pre-treatment workflow was shown in the left part of Fig. 1. Pre-treatment CT and MR simulations were acquired for each patient. In the study, the simulated CT (Philips Brilliance™, Netherland) and MRI (Philips Ingenia 3.0 T, Netherlands) were performed in supine position, with the slice thickness of 1 mm. The head immobilization mask and patient-specific polyurethane foam immobilization devices were used for body positioning. In accordance with the MRI scan protocol, the minimum imaging requirements consisted of a 3D T1/T2 weighted (T1w/T2w) scan (T1w: flip angle: 12°, TE: 2.4 ms, TR: 5.0 ms; T2w: flip angle: 120°, TE: 80 ms, TR: 6307 ms), gadolinium-enhanced T1 weighted (T1c) scan and fluid attenuated inversion recovery (Flair) scan (TE: 150 ms, TR: 12000 ms, TI: 2820 ms). All the images were transferred to Monaco treatment planning system (TPS) (v.5.40.02; Elekta AB, Stockholm, Sweden) for registering and delineating.

The delineation of brain lesions was evaluated by an experienced radiologist and a radiation oncologist before treatment. MRI T1c images and T2 images had been selected as the reference of gross tumor volume (GTV) delineation before FSRT (Fig. 2), while MRI T2 images (flip angle: 90°, TE: 182 ms, TR: 2100 ms) had been selected as the reference for adaptive GTV delineation during FSRT on the 1.5 T MR-Linac. The GTV

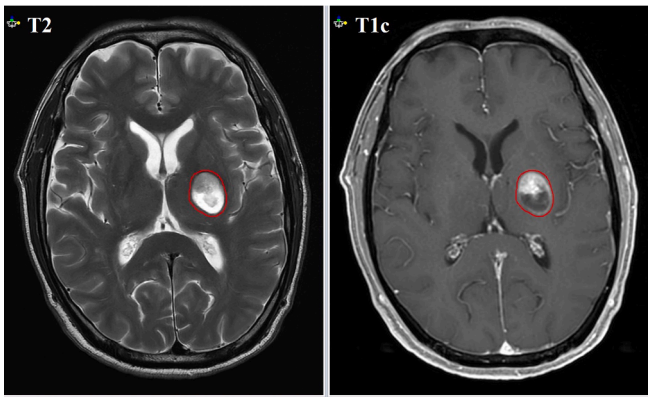

Fig. 2. The gross tumor volume delineation on MRI T2 and gadolinium-enhanced T1 weighted (T1c) images.

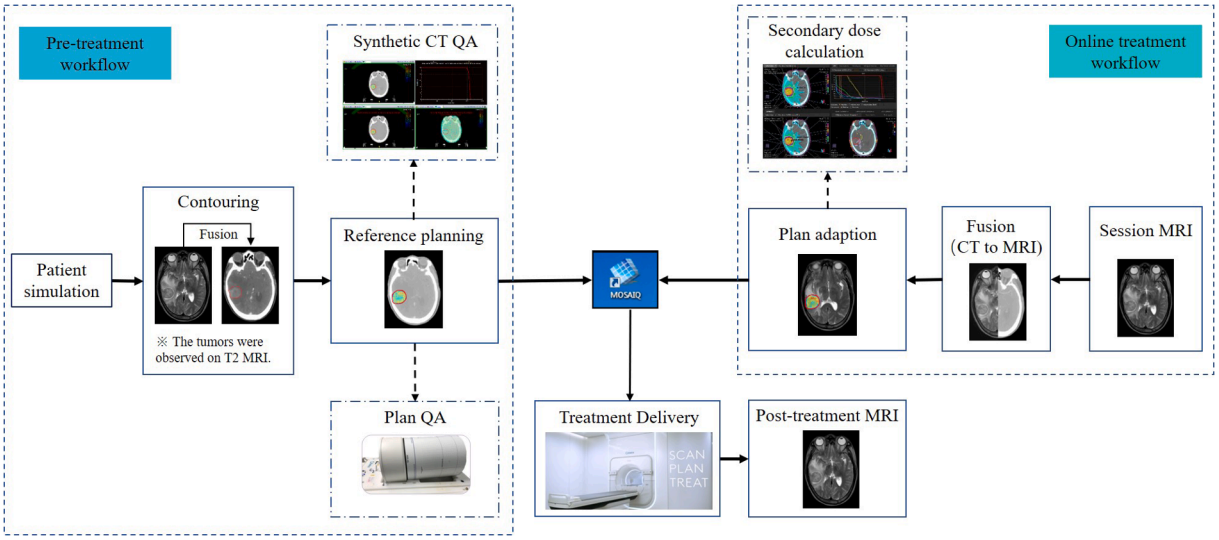

Fig. 1. The process for pre-treatment and online treatment workflow for MR-Linac.

and organs at risk (OARs) were delineated on the simulation CT imaging with visual support of the registered MR imaging. All GTV contours were delineated by 2 experienced radiation oncologists specialized in BMs in accordance with the international consensus contouring guideline. Standard planning target volume (PTV) margins expanded the GTV by 3 mm, depending on direction, and emulated the clinical standard at our institution.

A total dose of 30 Gy in 5 fractions had been prescribed to the PTV. The treatment plans satisfied that the prescribed dose covered the 95% volume of PTV and 99% volume of GTV, and the maximal dose was required be less than 110% of the prescribed dose. The dose constraints of OARs were referred to the ICRU report 83 [25] and the institutional guidelines on the dose criteria in FSRT planning for BMs. Regarding the OARs, the maximum doses to the lens, brain stem and optic nerves were set as 5 Gy, 30 Gy and 30 Gy. Additionally, the volume of brain stem receiving 20 Gy should be less than 30%.

The initial reference plans were optimized using 5–9 beam step-and-shoot intensity-modulated radiotherapy (IMRT) with a minimum number of 5 Monitor Units (MU) per segment, a minimum segment area of 2 cm^2, and a maximum of 100 segments. To consider the effect of the 1.5 T magnetic field, a graphic processing unit-based Monte Carlo dose engine (GPUMCD) [26] was applied in dose calculation with a dose grid size of 2 mm and a statistical uncertainty of 2% per control point. Besides, the anterior coil and the MR-Linac couch were considered in the dose calculation.

Before the treatment, a synthetic CT (sCT) quality assurance (QA) process was performed to assess the dose accuracy of bulk relative electron density (rED) assignment for online MRI based treatment plan. The dose accuracy was approved by an experienced medical physicist. Then, the reference plan was checked by a radiation oncologist and then transferred to the MOSAIQ system (Elekta AB, Stockholm, Sweden). All reference plans were proceeded by measurement-based pre-treatment verification using the ArcCheck MR (SunNuclear) to evaluate the dose delivery accuracy and to approve the treatment data transfer between the MR-Linac and the TPS.

Online treatment workflow

The online treatment workflow at each fraction was shown in the right part of Fig. 1. For the daily adapted plans, the session MRI was automatically imported into the online Monaco TPS. The rigid registration was automatically conducted between the planning CT and the session MRI. Manual adjustment was followed in this step if required. Then, Adapt to Position (ATP) or Adapt to Shape (ATS) workflow was applied according to the actual clinical condition. In the ATP process, the virtual couch shift was applied to match the current position of targets and OARs. In the ATS process, a new adapted plan was generated to match the anatomy of the day [27].

The online plan was evaluated and approved by a radiation oncologist. Meanwhile, a second planning system (Raystation) performed an independent dose calculation check without the magnetic field effect to assess great changes of the adapted plan [28]. After checking, the adapted plan was transferred to the MOSAIQ system and imported into the Unity MR-Linac. After beam on, the post-treatment MRI was acquired.

Dosimetric and geometrical analyses

GTV contouring variability and evaluation

The GTV was delineated on MRI T2 imaging at all fractions during FSRT to assess the changes at each fraction (Fx1, Fx2, Fx3, Fx4 and Fx5). The delineations were rigidly propagated to the pre-treatment simulation images (Fx0). The following metrics were applied to quantify the variability of GTV and edema:

(1) Absolute and relative volumes of GTV and edema on all the MR images. Relative volume (ΔV) was defined as a percentage of the volume at each fraction relative to the volume in simulation images, with negative and positive values illustrating reduction and enlargement, respectively.

$$\Delta V = \frac{(V_{\text{daily}} - V_{\text{reference}})}{V_{\text{reference}}} \times 100\%$$

(2) Dice similarity coefficient (DSC) delivered the ratio of overlap between daily and reference contours at CT and session MR image. The DSC is calculated as:

$$DSC = \frac{2(V_A \bigcap V_B)}{V_A + V_B}$$

where $V_A \bigcap V_B$ is the intersection of regions A and B. The DSC ranges from 0 to 1 where a higher value indicates a larger volume overlap.

(3) Hausdorff distance (HD) metrics delivered the greatest distance between daily and reference contours. Given two regions A and B, HD is defined as:

$$HD(A,B) = max[h(A,B), h(B,A)]$$

$$h(A,B) = \max_{a \in A} \min_{b \in B} \|a - b\|$$

Essentially, the HD describes the most mismatched distance of a point from A to B. If HD (A, B) = d, for instance, then every point within A must be within distance d of the nearest point with B and vice versa.

Dosimetric variability and assessment

Adaptive radiotherapy (ART) treatment plans were generated with the daily MRI datasets. The delineations and electron density information of the reference plan were propagated to the daily MRI and subsequently modulated by the physician and physicist to ensure the accuracy of daily delineations and electron density map. Based on the session MRI and adapted contours, the reference plan was modified according to the daily anatomy with the same optimization constraints and beam angles. The GTV was directly optimized in ART treatment plan. This was motivated by the potential reduction of treatment uncertainties with the online MR-Linac workflow that would incorporate high soft-tissue contrast MR images, accurate delineation of critical structures and adaptation of treatment plan before each fraction.

To create the non-ART treatment plans, the reference plan generated based on the PTV was exported into the daily MRI datasets. The radiation oncologists and physicists edited and ensured target delineations and electron density map. The reference plan was recalculated on the daily anatomy. For each patient, the differences in PTV and GTV coverage and dose to OARs between the adaptive and non-adaptive treatment plans were compared for each treatment session. The doses to whole brain in the two different plans were also calculated and evaluated.

Data statistics

The mean and standard deviation (SD) or rang and median were used to describe continuous data, and frequency counts and percentages were used to describe categorical data. All analyses were performed using SPSS (v25.0) (IBM Corporation, Armonk, NY, USA). Statistical analysis was carried out using Wilcoxon signed rank test and $p < 0.05$ was defined as the threshold for statistically significant.

Results

Patient and lesion characteristics

The baseline characteristics were summarized in Table 1. Twenty-eight patients with 88 brain metastatic lesions were analyzed. The median age was 61 years (range, 38 ~ 72 years) at diagnosis of BMs. There were 82.1% patients with primary lung adenocarcinoma. Fifteen

Table 1
Patient and tumor characteristics.

Characteristics	Patient Number (n = 28)
Age at BM diagnosis (Median, range)	61 (38–72)
Gender	
Female	9 (32.1%)
Male	19 (67.9%)
ECOG score	
0	8 (28.6%)
1	20 (71.4%)
Tumor histology	
Lung adenocarcinoma	23 (82.1%)
Small cell lung cancer	1 (3.6%)
Colon cancer	1 (3.6%)
Breast cancer	1 (3.6%)
Liver cancer	1 (3.6%)
Meningiomas	1 (3.6%)
Subtype of BM lesions	
Single	15 (53.6%)
Multiple	13 (46.4%)
Neurologic symptoms	
Yes	16 (57.1%)
No	12 (42.9%)
Perilesional edema	
Yes	14 (50%)
No	14 (50%)
Volume of lesions	0.071 ~ 39.007 cm^3

(53.6%) patients had single brain lesion and thirteen (46.4%) patients had multiple brain lesions. There were fifteen patients (57.1%) had neurologic symptoms.

Inter-fractional changes of every single lesion (n = 88)

There was a total of 88 lesions analyzed in this study. And the inter-fractional changes of every single lesion for each treatment fraction were showed in Fig. 3A and B. The median pre-treatment GTV was 1.171 cm^3 (range, 0.071 ~ 39.007 cm^3; interquartile [IQR], 0.459 cm^3). Compared to Fx0, the median inter-fractional volume reductions at Fx1, Fx2, Fx3, Fx4, and Fx5 were −0.75% (range, −74.48%~79.63%; IQR, −5.38%), −5.33% (range, −76.91%~135.19%; IQR, −13.99%), −9.32% (range, −78.31%~117.284%; IQR, −16.54%), −17.96% (range, −79.69% ~38.89%; IQR, −29.76%) and −27.73% (range, −79.69%~42.59%), respectively (Fig. 3A). Compared to Fx0, the shrinkage of GTV was statistically significant at Fx2, Fx3, Fx4 and Fx5 ($p < 0.045$, $p < 0.001$, $p < 0.001$ and $p < 0.001$).

The mean DSC index of GTV was 0.88 (range, 0.02 ~ 1), 0.81 (range, 0.01 ~ 0.99), 0.80 (rang, 0.08 ~ 0.99), 0.75 (range, 0.02 ~ 0.99) and 0.70 (range, 0 ~ 0.99) at Fx1, Fx2, Fx3, Fx4 and Fx5, respectively. Additionally, 16 (19%), 31 (35%), 33 (38%), 44 (50%) and 57 (65%) lesions had DSC < 0.8 at Fx1, Fx2, Fx3, Fx4 and Fx5, respectively.

The mean HD of GTV was 1.93 mm (range, 0 ~ 10.05 mm), 3.04 mm (range, 0.49 ~ 12.56 mm), 3.16 mm (rang, 0.49 ~ 13.17 mm), 3.69 mm (range, 0.51 ~ 12.71 mm) and 4.24 mm (range, 0.53 ~ 12.85 mm) at Fx1. Fx2, Fx3, Fx4 and Fx5, respectively. In addition, 26 (30%), 39 (44%), 47 (53%), 49 (56%) and 58 (66%) lesions had HD > 3 mm at Fx1, Fx2, Fx3, Fx4 and Fx5, respectively.

Inter-fractional changes of perilesional edema

There were 47 lesions in 14 patients with perilesional edema. The median volume of the perilesional edema at Fx0 was 7.04 cm^3 (range, 1.32 ~ 189.07 cm^3; IQR, 3.74 cm^3), and the changes of perilesional edema were shown in Fig. 4A and C. Compared to Fx0, the median inter-fractional changes of relative volume of perilesional edema at Fx1, Fx2, Fx3, Fx4, and Fx5 were 0.51% (range, −26.4%~9.29%; IQR, −1.17%), −4.96% (range, −39.20%~8.04%; IQR, −12.01%), −8.52% (range, −27.85%~4.09%; IQR, −13.52%), −11.14% (range, −36.36% ~16.52%; IQR, −13.58%) and −39.32% (range, −92.24%~40.89%; IQR, −56.51%), respectively.

The mean DSC index of perilesional edema was 0.91 (range, 0.76 ~ 0.97), 0.83 (range, 0.56 ~ 0.94), 0.79 (range, 0.49 ~ 0.93), 0.76 (rang, 0.51 ~ 0.91) and 0.67 (range, 0.27 ~ 0.85) at Fx1, Fx2, Fx3, Fx4 and Fx5, respectively.

The mean HD of perilesional edema was 4.36 mm (range, 1.75 ~ 15.56 mm), 5.65 mm (range, 1.76 ~ 15.82 mm), 6.33 mm (range, 1.76 ~ 18.78 mm), 6.63 mm (rang, 2.54 ~ 18.78 mm) and 7.71 mm (range, 3.36 ~ 18.96 mm) at Fx1, Fx2, Fx3, Fx4 and Fx5, respectively.

As summarized in Fig. 4B, the inter-fractional volume changes of lesions with perilesional edema (−15.18% ± 27.47%) were greater than the lesions without perilesional edema (−7.38% ± 16.78%), with $p < 0.001$. The DSC for the lesions with or without perilesional edema was significantly different, with 0.74 ± 0.20 and 0.83 ± 0.11, respectively ($p < 0.001$). The HD of lesions with perilesional edema was also larger than the lesions without perilesional edema (4.01 ± 2.67 mm vs 3.20 ± 2.39 mm, $p = 0.001$).

Inter-fractional changes of patients with single/multiple lesions

There were 15 patients had single lesion and 13 patients had multiple lesions in the current study. Compared to Fx0, the inter-fractional volume changes of patients with single lesion were −9.18% ± 12.23%. And the inter-fractional volume changes of patients with multiple lesions were −12.23% ± 23.34%. The volume changes were more significant for patients with multiple lesions ($p = 0.001$). The DSC of patients with single/multiple lesions was 0.84 ± 0.13 and 0.77 ± 0.17, respectively ($p = 0.01$). In addition, the HD of patients with single/multiple lesions was 2.89 ± 1.92 mm and 3.67 ± 2.84 mm, respectively ($p < 0.001$, Fig. 5A). Illustrative representative relationships between the initial and daily GTV for a multiple-lesions patient are shown in Fig. 5B.

Dosimetric variability and assessment

There were 140 non-adaptive and 140 adaptive plans during MR-guided FSRT were analyzed in 28 patients, as shown in Fig. 6A and B. For the 140 non-adaptive plans, there were 26 (19%) failing the PTV coverage constraints ($V_{100\%} \geq 95\%$), with 23 plans (16%) failing by more than 5% and 12 plans (9%) failing by more than 10% of prescribed dose coverage. Moreover, there were 20 plans (14%) failing the GTV coverage ($V_{100\%} \geq 99\%$), with 10 plans (7%) failing by more than 2% and 4 plans (3%) failing by more than 5% of prescribed dose coverage.

For the 140 adaptive plans, all the GTV coverage was maintained with coverage higher than 99.0% for the adaptive planning (Fig. 6A). The dose to OARs were similar for both adaptive and non-adaptive plans. Additionally, the irradiation dose to whole brain was also compared between adaptive and non-adaptive plans. The V_{3Gy}, V_{5Gy}, V_{10Gy} and V_{15Gy} of whole brain for non-adaptive plans were 24.46% ± 14.64%, 17.83% ± 12.88%, 8.20% ± 9.41% and 4.41% ± 6.22%, respectively. Furthermore, the V_{3Gy}, V_{5Gy}, V_{10Gy} and V_{15Gy} of whole brain for adaptive plans were 20.67% ± 13.76%, 14.46% ± 12.02%, 6.27% ± 8.25% and 3.22% ± 5.06%, respectively. Comparing to the non-adaptive plans, the adaptive plans had lower dose to whole brain ($p < 0.001$). Illustrative representative changes between the ART and non-ART plans are shown in Fig. 6C.

Discussion

This study reported the inter-fractional changes of 88 brain metastatic lesions in 28 patients treated with MR-guided FSRT and analyzed the necessity for adaptive plans. Significant tumor volume reduction had been found during FSRT compared to Fx0 for all 88 lesions (median −0.75%, −5.33%, −9.32%, −17.96% and −27.73% at Fx1, Fx2, Fx3, Fx4 and Fx5, $p < 0.05$). There were 47 (47/88, 53.4%) lesions being accompanied by perilesional edema and the inter-fractional changes were significantly different compared to those without perilesional

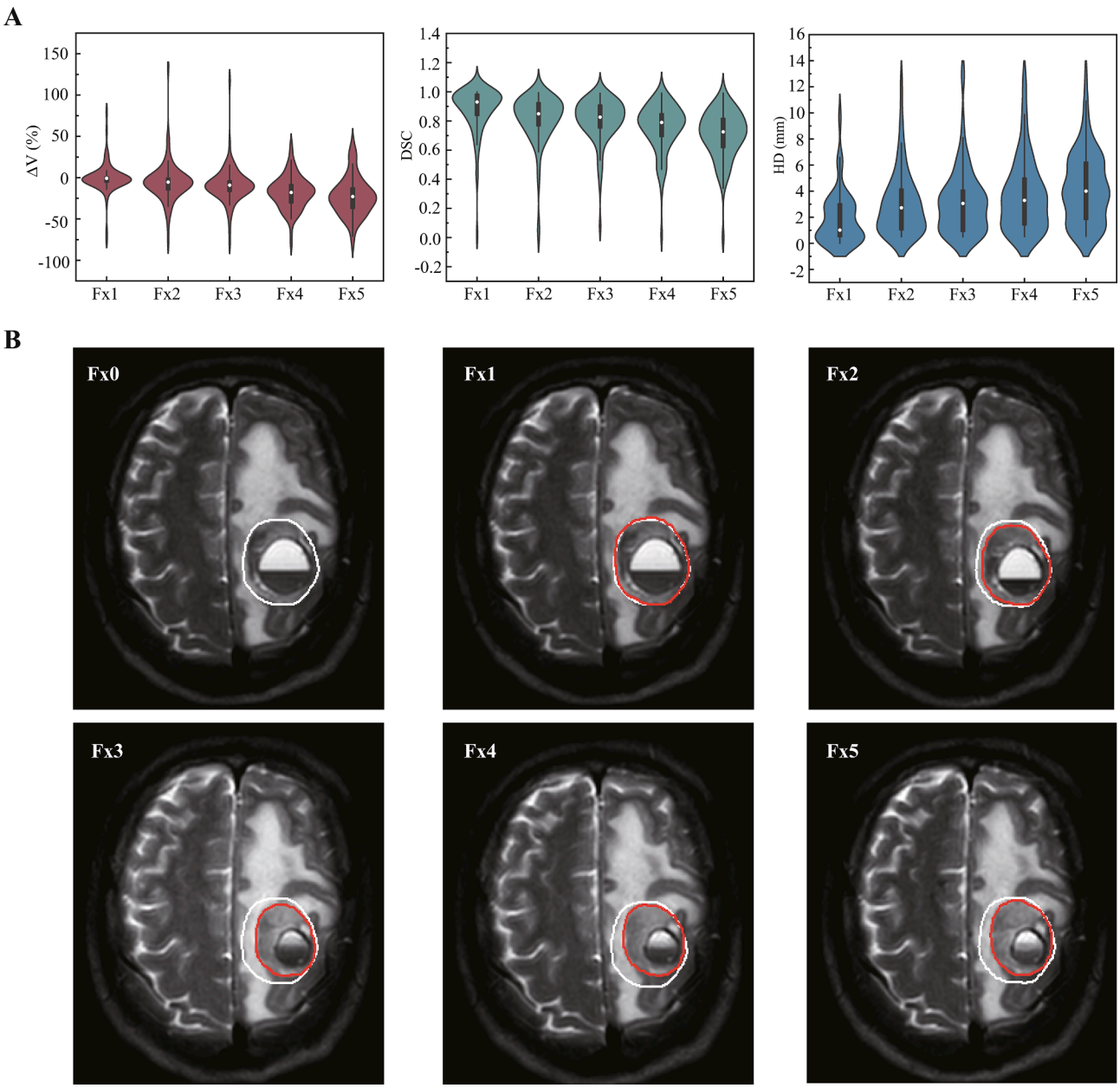

Fig. 3. Inter-fractional changes of gross target volume for all the brain lesions. (A) The ΔV, DSC and HD of GTV at Fx1, Fx2, Fx3, Fx4 and Fx5 for all the brain lesions (n = 88). (B) Axial slices of a case at planning (Fx0), fraction 1, 2, 3, 4 and 5 (Fx1, Fx2, Fx3, Fx4 and Fx5), illustrating patient-specific serial gross tumor volume changes. The planned GTV (baseline, Fx0) was contoured in white-line and the GTVs from daily MR scans (Fx1-5) were in red-line; the Fx0 delineation was also interpolated post registration to daily MRI for comparison migration. (For interpretation of the references to colour in this figure legend, the reader is referred to the web version of this article.)

edema ($p < 0.001$). Patients with multiple lesions (13/28, 46.4%) had more significant inter-fractional tumor changes than those with single lesion (15/28, 53.6%), including tumor volume reduction and anatomical shift ($p < 0.001$). PTV coverage of non-adaptive plans was below the prescribed coverage in 26/140 fractions (19%), with 12 (9%) failing by more than 10%. All 140 adaptive fractions met prescribed target coverage. The adaptive plans also had lower dose to whole brain than non-adaptive plans ($p < 0.001$).

Several studies showed the changes in tumor size and position between planning/diagnostic MRI and the images acquired before stereotactic radiosurgery for patients with BMs [29,30]. However, few studies focused on the continuous changes of lesions caused by FSRT [8,9]. Our study showed that metastatic brain lesions had significant volume reduction during FSRT, with median relative reduction volume of −27.73% at Fx5 compared to Fx0. The change of tumor volume was not symmetric (Fig. 3), which implied that inter-fractional MRI was necessary and adaptive plan could be helpful to reduce the radiation induced toxicity. A recent study found that the PTV size of brain lesions changed up to 43.0% during the whole course of FSRT [2]. Great conformity and a relatively small margin of PTV were required for FSRT, therefore, the reduction in tumor volume might bring extra radiation to normal structure or insufficient dose coverage of GTV and PTV.

Among the 88 lesions, there were 47 with perilesional edema. As is well known, perilesional brain edema could affect intracranial pressure and cause serious complications in the management of patients with BMs. The current study showed that significant reduction of the volume of perilesional edema during MR-guided FSRT, which could lead to distinct neurologic symptom improvement and promising intracranial

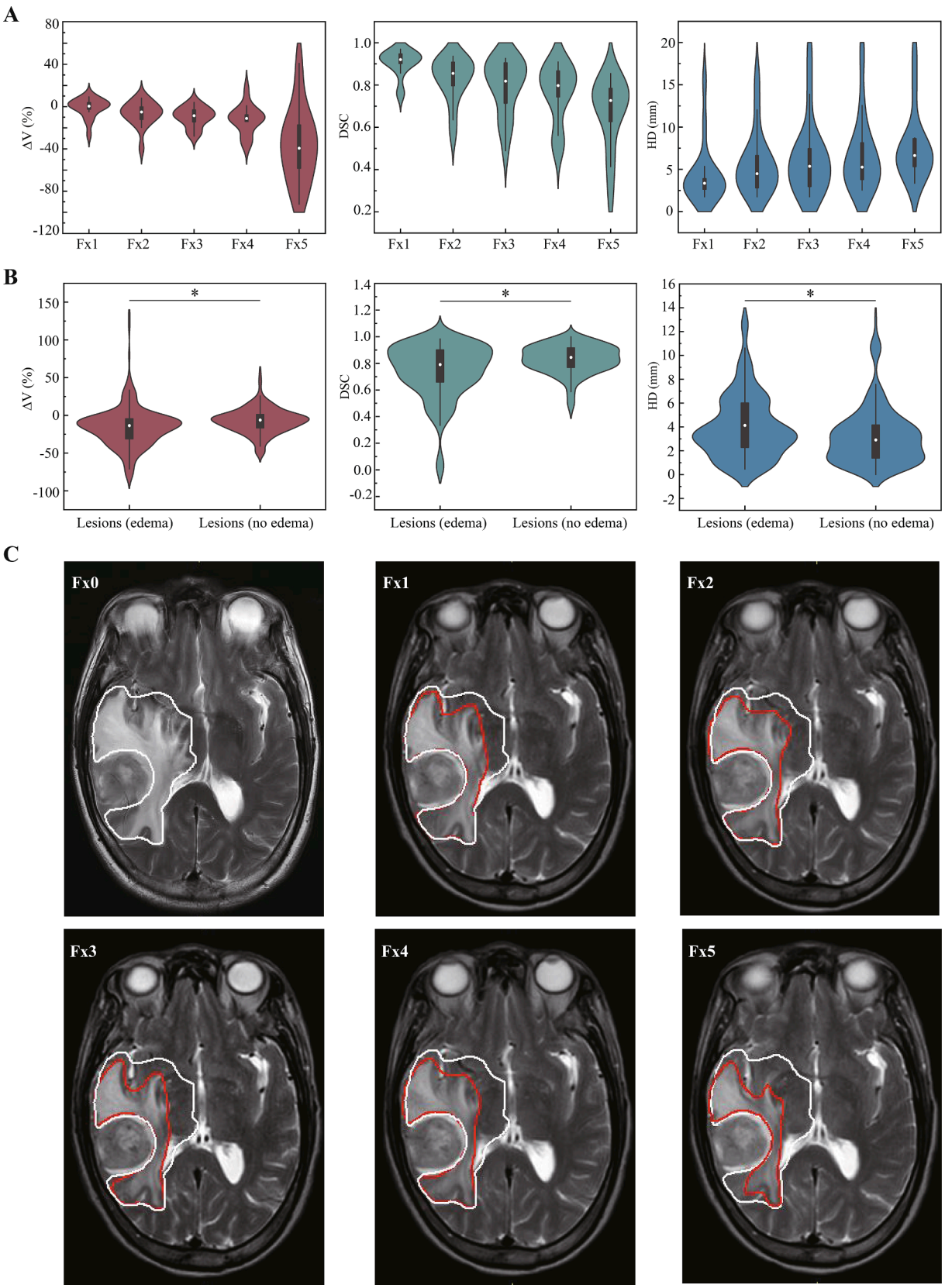

Fig. 4. Inter-fractional changes of perilesional edema. (A) The ΔV, DSC and HD of GTV at Fx1, Fx2, Fx3, Fx4 and Fx5 for the perilesional edema. (B) The differences of ΔV, DSC and HD of lesions with or without perilesional edema. A * indicates a significance of $p < 0.05$. (C) Axial slices of a case at planning (Fx0), fraction 1, 2, 3, 4 and 5 (Fx1, Fx2, Fx3, Fx4 and Fx5), illustrating patient-specific serial perilesional edema changes. The perilesional edema from planning imaging (baseline, Fx0) was contoured in white-line and the perilesional edema from daily MR scans (Fx1-5) were in red-line; the Fx0 delineation was also interpolated post-registration to daily MRI for comparison migration. (For interpretation of the references to colour in this figure legend, the reader is referred to the web version of this article.)

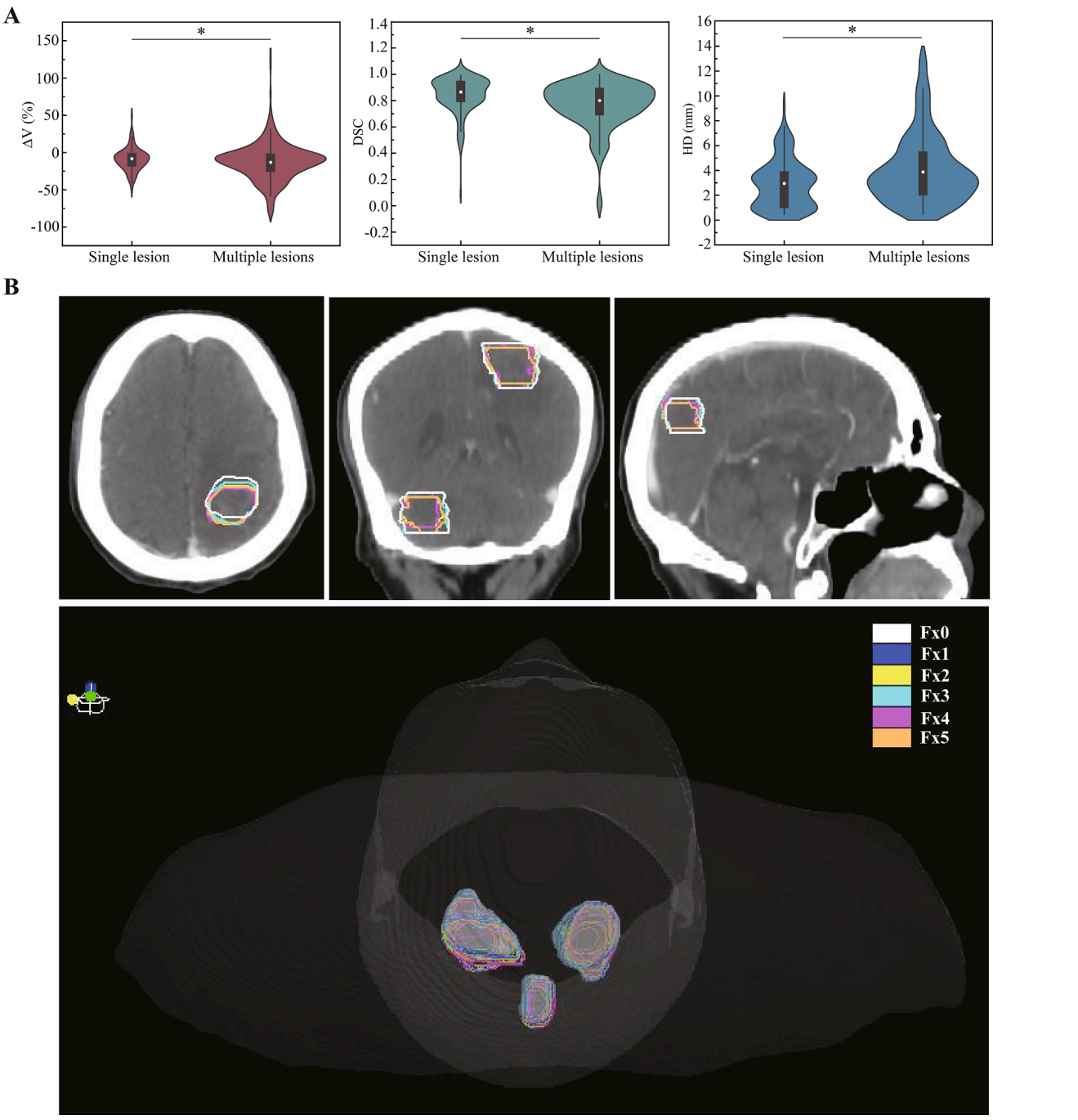

Fig. 5. Inter-fractional changes of patients with single/multiple lesions. (A) The differences of ΔV, DSC and HD of single and multiple lesions. A * indicates a significance of $p < 0.05$. (B) The gross tumor volume delineation and 3D projection charts of a multiple lesions patient at planning (Fx0), fraction 1, 2, 3, 4 and 5 (Fx1, Fx2, Fx3, Fx4 and Fx5) on initial CT, illustrating patient-specific serial multiple lesions volume changes and anatomical shifts.

disease control (Fig. 4). However, the changes of the perilesional edema volume were asymmetrical and irregular. Compared to the perilesional edema volume at Fx0 (median, 7.04 cm^3; range, 1.32 ~ 189.07 cm^3), the median inter-fractional changes at Fx1, Fx2, Fx3, Fx4 and Fx5 were 0.51%, −4.96%, −8.52%, −11.14% and −39.32%. The inter-fractional changes of lesions with perilesional edema were greater than the lesions without perilesional edema ($p < 0.001$). Recently, Hessen et al. explored the value of repeating MRI in 42 BMs treated by SRS. A notable reduction of up to 34.8% in target coverage was observed in patients with in situ BMs [30]. The application of MR-Linac provided information of GTV changes during FSRT courses of BMs with perilesional edema and showed significant clinical benefit from online adaptive MR-guided FSRT.

In current study, the inter-fractional changes were more significant in patients with multiple lesions than those with single lesion ($p < 0.001$). Not only tumor volume change but also the geometrical shift/rotation could increase the radiation dose to normal organs and lower the dose coverage of target. In this study, the maximal HD of GTV was 13.17 mm, which implied that even if there was no significant tumor volume reduction, the geometrical shift and rotation could occur and lead to insufficient dose coverage. This insufficient target coverage might be the reason for tumor recurrence after FSRT. For the 140 non-adaptive plans, there were 26 (19%) failing the PTV coverage constraints ($V_{100\%} \geq 95\%$), with 23 plans (16%) failing by more than 5%

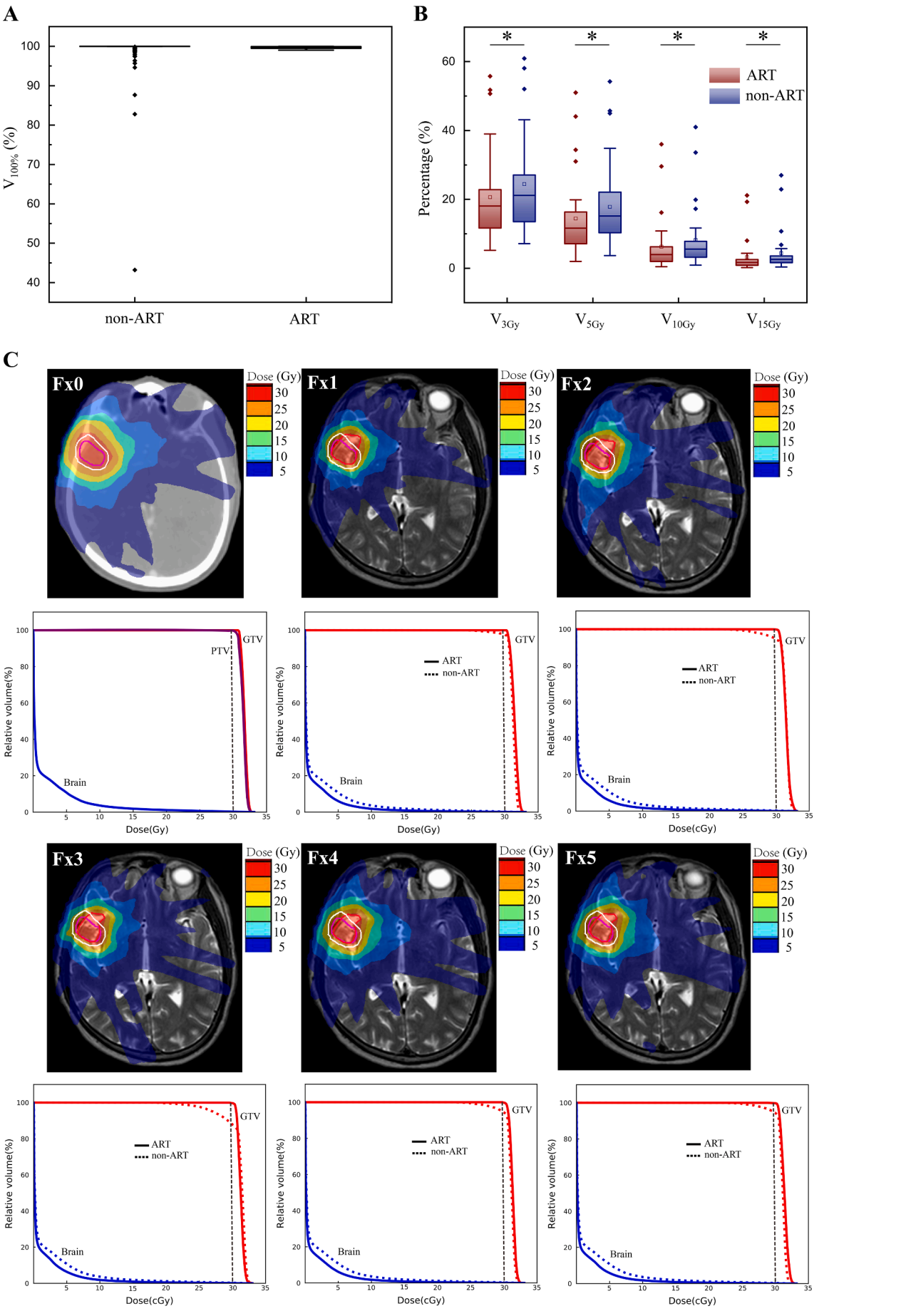

(caption on next page)

Fig. 6. The dose differences of ART and non-ART plans. (A) The GTV coverage between ART and non-ART plans. (B) The V_{3Gy}, V_{5Gy}, V_{10Gy} and V_{15Gy} of whole brain between ART and non-ART plans. A * indicates a significance of $p < 0.05$. (C) The dose mapping and dose volume histogram between ART and non-ART plans. The Fx0 PTV was contoured in white-line, the Fx0 GTV was contoured in pink-line, and the daily GTV was contoured in red-line. (For interpretation of the references to colour in this figure legend, the reader is referred to the web version of this article.)

and 12 plans (9%) failing by more than 10% of prescribed dose coverage. Moreover, there were 20 plans (14%) failing the GTV coverage ($V_{100\%} \geq 99\%$), with 10 plans (7%) failing by more than 2% and 4 plans (3%) failing by more than 5% of prescribed dose coverage. For the adaptive plans, all the GTV coverage was maintained with higher than 99.0% for the adaptive planning. Compared to the non-adaptive plans, the adaptive plans had lower median dose to whole brain ($p < 0.001$). Therefore, the daily MR-guided optimization during FSRT could be useful for patients with BMs. The lower dose to whole brain by adaptive plans might be able to reduce the incidence of radiation-induced cognitive impairment in patients with multiple lesions.

As mentioned above, the online adaptive MR-guided FSRT could be a useful treatment option for patients diagnosed with BMs. However, there were several limitations remaining in current study: 1. all the patients were treated in a single institution, and nearly 40% of them were previously treated with targeted treatment, chemotherapy and surgery; 2. FSRT was guided by MRI without contrast, therefore we only analyzed lesions that could be seen from T2w imaging; 3. An observation study with few patient numbers and events. These facts introduced potential biases.

In conclusion, significant gross tumor volume reductions and geometrical changes had been found during online adaptive MR-guided FSRT in patient with BMs. The changes in tumor were likely to occur even in a short period, and the adaptive plan was necessary during FSRT treatment. Online adaptive MR-guided FSRT by MR-Linac resulted in better target conformality, coverage and OAR sparing in patients with BMs. Significant dosimetric benefit was observed for patients with perilesional edema or multiple lesions, using daily MR-guided re-optimization of treatment plans. The data from this study warrants validation by further study with long-term follow-up.

Ethical approval and consent to participate

Ethics approval for this study was obtained from the Clinical Research Ethics Committee of Sun Yat-sen University Cancer Center approved this study (B2022-126–01). And all patients provided written informed consent prior to enrollment.

Availability of supporting data

Research data are stored in an institutional repository and will be shared upon request to the corresponding author.

Funding

This work was supported by the National Key R&D Program of China (No. 2022YFC2404604), National Natural Science Foundation of China (No. 12275372), Guangdong Basic and Applied Basic Research Foundation (No. 2023A1515011153), Guangdong Basic and Applied Basic Research Guangdong-Guangzhou Joint Youth Fund (No. 2021A1515110642), and Tumor Precision Radiotherapy Summit Program Clinical Research Fund Project (No. 2021-DF-009).

Declaration of Competing Interest

The authors declare that they have no known competing financial interests or personal relationships that could have appeared to influence the work reported in this paper.

References

[1] Suh JH. Stereotactic radiosurgery for the management of brain metastases. N Engl J Med 2010;362(12):1119–27.
[2] Kubo K, Kenjo M, Doi Y, Nakao M, Miura H, Ozawa S, et al. MRI appearance change during stereotactic radiotherapy for large brain metastases and importance of treatment plan modification during treatment period. Jpn J Radiol 2019;37(12):850–9.
[3] Lehrer EJ, Peterson JL, Zaorsky NG, Brown PD, Sahgal A, Chiang VL, et al. Single versus multifraction stereotactic radiosurgery for large brain metastases: an international meta-analysis of 24 trials. Int J Radiat Oncol Biol Phys 2019;103(3):618–30.
[4] Angelov L, Mohammadi AM, Bennett EE, Abbassy M, Elson P, Chao ST, et al. Impact of 2-staged stereotactic radiosurgery for treatment of brain metastases ≥ 2 cm. J Neurosurg 2018;129(2):366–82.
[5] Fiorentino A, Giaj-Levra N, Tebano U, Mazzola R, Ricchetti F, Fersino S, et al. Stereotactic ablative radiation therapy for brain metastases with volumetric modulated arc therapy and flattening filter free delivery: feasibility and early clinical results. Radiol Med 2017;122(9):676–82.
[6] Hasegawa T, Kato T, Yamamoto T, Lizuka H, Nishikawa T, Ito H, et al. Multisession gamma knife surgery for large brain metastases. J Neurooncol 2017;131(3):517–24.
[7] Dohm A, McTyre ER, Okoukoni C, Henson A, Cramer CK, Lecompte MC, et al. Staged stereotactic radiosurgery for large brain metastases: local control and clinical outcomes of a one-two punch technique. Neurosurgery 2018;83(1):114–21.
[8] Lee MH, Kim KH, Cho KR, Choi JW, Kong DS, Seol HJ, et al. Volumetric changes of intracranial metastases during the course of fractionated stereotactic radiosurgery and significance of adaptive planning. J Neurosurg 2019:1–6.
[9] Hessen E, Nijkamp J, Damen P, Hauptmann M, Jasperse B, Dewit L, et al. Predicting and implications of target volume changes of brain metastases during fractionated stereotactic radiosurgery. Radiother Oncol 2020;142:175–9.
[10] Soliman H, Ruschin M, Angelov L, Brown PD, Chiang VLS, Kirkpatrick JP, et al. Consensus contouring guidelines for postoperative completely resected cavity stereotactic radiosurgery for brain metastases. Int J Radiat Oncol Biol Phys 2018;100(2):436–42.
[11] Maziero D, Straza MW, Ford JC, Bovi JA, Diwanji T, Stoyanova R, et al. MR-guided radiotherapy for brain and spine tumors. Front Oncol 2021;11:626100.
[12] Narita Y, Sato S, Kayama T. Review of the diagnosis and treatment of brain metastases. Jpn J Clin Oncol 2022;52(1):3–7.
[13] Yuan J, Law SCK, Wong KK, Lo GG, Kam MKM, Kwan WH, et al. 3D T1-weighted turbo spin echo contrast-enhanced MRI at 1.5 T for frameless brain metastases radiotherapy. J Cancer Res Clin Oncol 2022;148(7):1749–59.
[14] Uto M, Ogura K, Katagiri T, Takehana K, Mizowaki T. Interfractional target changes in brain metastases during 13-fraction stereotactic radiotherapy. Radiat Oncol 2021;16(1):140.
[15] Kawashima M, Akabane A, Noda R, Segawa M, Tsunoda S, Inoue T. Interfractional change of tumor volume during fractionated stereotactic radiotherapy using gamma knife for brain metastases. J Neurooncol 2022;159(2):409–16.
[16] Hall WA, Paulson ES, van der Heide UA, Fuller CD, Raaymakers BW, Lagendijk JJW, et al. The transformation of radiation oncology using real-time magnetic resonance guidance: A review. Eur J Cancer 2019;122:42–52.
[17] Cao Y, Tseng CL, Balter JM, Teng F, Parmar HA, Sahgal A. MR-guided radiation therapy: transformative technology and its role in the central nervous system. Neuro Oncol 2017;19(suppl_2):ii16–29.
[18] Putz F, Mengling V, Perrin R, Masitho S, Weissmann T, Rosch T, et al. Magnetic resonance imaging for brain stereotactic radiotherapy : A review of requirements and pitfalls. Strahlenther Onkol 2020;196(5):444–56.
[19] Lagendijk JJ, van Vulpen M, Raaymakers BW. The development of the MRI linac system for online MRI-guided radiotherapy: a clinical update. J Intern Med 2016;280(2):203–8.
[20] Acharya S, Fischer-Valuck BW, Mazur TR, Curcuru A, Sona K, Kashani R, et al. Magnetic resonance image guided radiation therapy for external beam accelerated partial-breast irradiation: evaluation of delivered dose and intrafractional cavity motion. Int J Radiat Oncol Biol Phys 2016;96(4):785–92.
[21] Tseng CL, Stewart J, Whitfield G, Verhoeff JJC, Bovi J, Soliman H, et al. Glioma consensus contouring recommendations from a MR-Linac International Consortium Research Group and evaluation of a CT-MRI and MRI-only workflow. J Neurooncol 2020;149(2):305–14.
[22] Finazzi T, Palacios MA, Haasbeek CJA, Admiraal MA, Spoelstra FOB, Bruynzeel AME, et al. Stereotactic MR-guided adaptive radiation therapy for peripheral lung tumors. Radiother Oncol 2020;144:46–52.
[23] Intven MPW, de Mol van Otterloo SR, Mook S, Doornaert PAH, de Groot-van Breugel EN, Sikkes GG, et al. Online adaptive MR-guided radiotherapy for rectal cancer; feasibility of the workflow on a 1.5T MR-linac: clinical implementation and initial experience. *Radiother Oncol* 2021, 154:172-178.
[24] Lagendijk JJ, Raaymakers BW, Raaijmakers AJ, Overweg J, Brown KJ, Kerkhof EM, et al. MRI/linac integration. Radiother Oncol 2008;86(1):25–9.

[25] Hodapp N. The ICRU Report 83: prescribing, recording and reporting photon-beam intensity-modulated radiation therapy (IMRT). Strahlenther Onkol 2012;188(1):97–9.
[26] Hissoiny S, Raaijmakers AJ, Ozell B, Despres P, Raaymakers BW. Fast dose calculation in magnetic fields with GPUMCD. Phys Med Biol 2011;56(16):5119–29.
[27] Bertelsen AS, Schytte T, Møller PK, Mahmood F, Riis HL, Gottlieb KL, et al. First clinical experiences with a high field 1.5 T MR Linac. Acta Oncol 2019;58(10):1352–7.
[28] Li Y, Wang B, Ding S, Liu H, Liu B, Xia Y, et al. Feasibility of using a commercial collapsed cone dose engine for 1.5T MR-LINAC online independent dose verification. Phys Med 2020;80:288–96.
[29] Salkeld AL, Hau EKC, Nahar N, Sykes JR, Wang W, Thwaites DI. Changes in brain metastasis during radiosurgical planning. Int J Radiat Oncol Biol Phys 2018;102(4):727–33.
[30] Hessen ED, van Buuren LD, Nijkamp JA, de Vries KC, Mok WK, Dewit L, et al. Significant tumor shift in patients treated with stereotactic radiosurgery for brain metastasis. Clin Transl Radiat Oncol 2017;2:23–8.